Inhibition of cholesterol biosynthesis disrupts lipid raft/caveolae and affects insulin receptor activation in 3T3-L1 preadipocytes

Jana Sánchez-Wandelmer [a], Alberto Dávalos [a], Emilio Herrera [b], Martin Giera [c], Sonia Cano [a], Gema de la Peña [a], Miguel A. Lasunción [a,d,e], Rebeca Busto [a,e,*]

[a] Servicio de Bioquímica-Investigación, Hospital Ramón y Cajal, Madrid, Spain
[b] Faculties of Pharmacy and Medicine, Universidad San Pablo Centro de Estudios Universitarios (CEU), Madrid, Spain
[c] Department Pharmazie, Ludwig Maximilians Universität München, Munich, Germany
[d] Departamento de Bioquímica y Biología Molecular, Universidad de Alcalá, Madrid, Spain
[e] CIBER de la Fisiopatología de la Obesidad y Nutrición (CIBEROBN), ISCIII, Spain

ARTICLE INFO

ABSTRACT

Lipid rafts are plasma membrane microdomains that are highly enriched with cholesterol and sphingolipids and in which various receptors and other proteins involved in signal transduction reside. In the present work, we analyzed the effect of cholesterol biosynthesis inhibition on lipid raft/caveolae composition and functionality and assessed whether sterol precursors of cholesterol could substitute for cholesterol in lipid rafts/caveolae. 3T3-L1 preadipocytes were treated with distal inhibitors of cholesterol biosynthesis or vehicle (control) and then membrane rafts were isolated by sucrose density gradient centrifugation. Inhibition of cholesterol biosynthesis with either SKF 104976, AY 9944, 5,22-cholestadien-3β-ol or triparanol, which inhibit different enzymes on the pathway, led to a marked reduction in cholesterol content and accumulation of different sterol intermediates in both lipid rafts and non-raft domains. These changes in sterol composition were accompanied by disruption of lipid rafts, with redistribution of caveolin-1 and Fyn, impairment of insulin-Akt signaling and the inhibition of insulin-stimulated glucose transport. Cholesterol repletion abrogated the effects of cholesterol biosynthesis inhibitors, reflecting they were specific. Our results show that cholesterol is required for functional raft-dependent insulin signaling.

© 2009 Elsevier B.V. All rights reserved.

1. Introduction

Cholesterol is an essential molecule in animals, serving as a principal component of plasma membranes, an obligatory precursor for the biosynthesis of steroid hormones, bile acids, and bioactive oxysterols, and also exerting regulatory functions. Cholesterol biosynthesis involves successive enzymatic reactions that first convert acetyl-CoA into the 30-carbon molecule squalene, then cycle that molecule to yield the first sterol, lanosterol, and finally, through additional 18 enzymatic reactions including 3 demethylations and double-bond reorganizations, generate cholesterol (Fig. 1).

Lipid rafts are plasma membrane microdomains that are highly enriched with cholesterol and sphingolipids [1]. Caveolae are considered as a subtype of lipid raft that are formed in cells expressing caveolin [2]. Lipid rafts/caveolae have been shown to be involved in endocytosis/transcytosis, cholesterol transport, tumorigenesis, and regulation of signal transduction [2–5].

Various signaling molecules and receptors are recruited into caveolae by caveolins through their scaffolding domain [6]. Bringing these signaling molecules into close proximity enables efficient signal transduction [7]. The insulin receptor (IR) and many molecules involved in the IR signaling cascade have been shown to concentrate in caveolin-enriched plasma membrane domains from adipocytes [8–10], a finding that could not be confirmed in other studies [11]. Caveolin-1 is phosphorylated by the IR [10] and functions as an activator of IR signaling [12]. In fact, both caveolin-1-deficient mice and caveolin-3 knockout mice suffer from insulin resistance [13,14]. Very recently, the cavin-knockout mouse, which lacks morphologically detectable caveolae and markedly diminished protein expression of the three caveolin isoforms, has been reported to have glucose intolerance and hyperinsulinemia [15], all of which underscore the role of caveolae in insulin action.

Cholesterol appears to be essential for the stability and functionality of lipid rafts/caveolae. Inhibition of 3-hydroxy-3-methylglutaryl-CoA-reductase (HMG-CoA reductase) by statins [16,17] or membrane cholesterol depletion using methyl-cyclodextrin [8,18,19] resulted in lipid raft disruption, modification of lipid raft composition, and inhibition of cell signaling. Likewise, RNA interference-mediated inhibition of squalene synthase affected several cell functions by selectively reducing the cholesterol content of lipid rafts [20].

* Corresponding author. Servicio de Bioquímica-Investigación, Hospital Ramón y Cajal, Ctra. de Colmenar km. 9, E-28034, Madrid, Spain. Tel.: +34 91 336 8077; fax: +34 91 336 9016.
E-mail address: rebeca.busto@hrc.es (R. Busto).

Fig. 1. Scheme of the cholesterol biosynthesis pathway showing the enzymes inhibited by SKF 104976, AY 9944, 5,22-cholestadien-3β-ol, and triparanol.

The presence of biosynthetic sterol intermediates in plasma membranes is well described [21] but their distribution into lipid raft and non-raft areas of the membrane and their role in caveolae function are not well understood. Their properties in stabilizing rafts have been studied in membrane models. 7-Dehydrocholesterol (7DHC) promotes liquid-ordered domain formation more strongly than cholesterol [22], but has a markedly different effect on membrane organization and dynamics [23]. However, more proximal sterol intermediates stabilize raft formation weakly [24]. Lateral pressure, which plays a significant role in the activation of membrane proteins, is altered when cholesterol is replaced by either desmosterol or 7DHC [25].

In rats treated with AY9944, a Δ^7-reductase inhibitor, 7DHC has been shown to incorporate into lipid rafts as efficiently as cholesterol but the raft protein content was perturbed [26]. Desmosterol may replace cholesterol in the formation of unilamellar vesicles with phospholipids [27]; however, in mammalian cell membranes, exchanging cholesterol for desmosterol leads to impaired raft-dependent signaling [28,29]. Likewise, desmosterol-reductase-deficient fibroblasts, which accumulate desmosterol in membranes instead of cholesterol, have disrupted caveolae and impaired insulin-Akt-Bad signaling [7].

In the present work, to study the effects of cholesterol deprivation and to explore whether sterol precursors could substitute for cholesterol in lipid rafts/caveolae, we treated 3T3-L1 preadipocytes with different inhibitors acting on the conversion of lanosterol into cholesterol. The results show that inhibition of cholesterol biosynthesis causes marked reductions in cholesterol content and accumulation of sterol intermediates in both raft and non-raft membrane domains. This is accompanied by disruption of lipid rafts/caveolae, redistribution of caveolin-1, and impairment of insulin signaling. The results of our study demonstrate the stringency of the sterol requirement of lipid rafts/caveolae for insulin receptor activation in 3T3-L1 preadipocytes.

2. Materials and methods

All chemicals, unless otherwise stated, were purchased from Sigma (Sigma-Aldrich Química, S.A., Tres Cantos, Madrid, Spain).

2.1. Culture of 3T3-L1 cells

3T3-L1 preadipocyte cells (ATCC CL-173) (Rockville, MD, USA) were cultured in DMEM supplemented with 10% fetal bovine serum (FBS) and antibiotics (Gibco BRL, Invitrogen S.A., Prat de Llobregat, Barcelona, Spain) at 37 °C in a 5% CO_2 atmosphere. For experiments, cells were cultured in DMEM with 10% lipoprotein-deficient serum (LPDS) and treated with the drugs for 24 h. LPDS was prepared from FBS by ultracentrifugation at a density of 1.21 kg/L. Sterols (cholesterol and 5,22-cholestadien-3β-ol, [Steraloids Inc., Newport, RI, USA]) were dissolved in ethanol; cholesterol biosynthesis inhibitors (SKF 104976 [GlaxoSmithKline plc., Brentford, Middlesex, United Kingdom], AY 9944 [Wyeth-Ayerst Research, Wyeth Madison, NJ, USA], and triparanol [Sigma]) were dissolved in DMSO. The final concentrations of DMSO and ethanol in the medium were 0.044% and 0.44%, respectively.

The following inhibitors of cholesterol biosynthesis were used at the indicated doses: 3 μM SKF 104976 (an inhibitor of lanosterol 14α-demethylase), 5 μM AY 9944 (an inhibitor of 3β-hydroxysterol Δ^7-reductase), 1 μg/mL 5,22-cholestadien-3β-ol (an inhibitor of sterol Δ^{24} reductase), and 3 μM triparanol (an inhibitor of sterol Δ^{24} reductase, as well as β-hydroxysterol Δ^7-reductase, $\Delta^{8,7}$-isomerase, and sterol Δ^{14}-reductase, depending on the dose). The effect of these compounds on cholesterol biosynthesis enzymes has been reported elsewhere [30–32]. The doses used were selected to achieve maximal inhibition of ^{14}C-acetate incorporation into cholesterol (Supplemental results and Supplementary Fig. 1).

2.2. Cell viability measurement

Mitochondrial activity was analyzed with the MTT assay (cell proliferation kit I (MTT); Boehringer-Mannheim [Barcelona, Spain]) in 3T3-L1 cells treated with or without cholesterol biosynthesis inhibitors (3 μM SKF 104976, 5 μM AY 9944, 1 μg/mL 5,22-cholestadien-3β-ol and 3 μM triparanol) during 24 h. The MTT assay determines the ability of cells to metabolize 3-(4,5-dimethylthiazol-2-yl)-2,5-diphenyl tetrazolium bromide (MTT). At the end of the cell treatment period, 300 μL of culture medium were removed from a total of 500 μL of each well and 20 μL of MTT solution (5 mg/mL) were added and incubated for 2 h. At this time, 200 μL of solubilization solution (10% SDS in HCl 0.01 M) was then added to the wells and after overnight incubation at 37 °C, 100 μL was transferred into 96-well microtiter plate, and the absorption value at 550 nm was measured in an automatic microtiter reader (Spectra Fluor, Tecan).

2.3. Immunofluorescence microscopy

3T3-L1 cells were cultured on glass coverslips, fixed with 4% paraformaldehyde/PBS for 5 min. Next, cells were permeabilized in 0.1% triton X-100/PBS for 5 min and blocked with 2% bovine serum albumin (BSA) in PBS for 45 min. Free cholesterol was stained with filipin (50 mg/L in PBS) for 45 min; caveolin-1 with anti-caveolin-1 (1:100, 2 h) (Santa Cruz Biotechnology, Santa Cruz, CA, USA) and Alexa fluor 488-conjugated anti-rabbit IgG (Molecular Probes, Invitrogen S.A.); and nuclei with 1 μM TO-PRO-3 (Molecular Probes) for 15 min. For GM1 staining, the cells were incubated with cholera toxin B-FITC (CtxB-FITC) (1:100) (Sigma) for 30 min before fixing. Cells were examined on an Olympus BX51 (Olympus España, S.A., Barcelona, Spain) reflected fluorescence microscope for filipin and caveolin or a Bio-Rad (Bio-Rad Laboratories S.A., El Prat de Llobregat, Barcelona, Spain) laser confocal fluorescence microscope for GM1 and caveolin. Images of filipin staining were pseudocolored in red.

2.4. Sucrose gradient fractionation of membranes

To separate membrane fractions we used a modified version of a previously described detergent-free method [33]. 3T3-L1 cells (175-mm flask) were scraped into 2 mL of 500 mM sodium carbonate, pH 11, sonicated 2 bursts of 30 s each and centrifuged for 30 min at 14,000 g to obtain a Golgi-free supernatant. Then Golgi-free supernatant proteins were measured by bicinchoninic acid (BCA) protein assay (Pierce Biotechnology, Inc., Rockford, IL, USA). Equal amounts of membrane proteins were then adjusted to 42.5% sucrose by the addition of 2 mL of 85% sucrose prepared in MBS (25 mM Mes, pH 6.5, 0.15 M NaCl) and placed at the bottom of an ultracentrifuge tube. A 5%–35% discontinuous sucrose gradient was formed above (2 mL of 5% sucrose, 5 mL of 30% sucrose, 1 mL of 35% sucrose) and centrifuged at 39,000 rpm for 18–20 h in an SW41 rotor (Beckman Instruments, Palo Alto, CA, USA). Twelve 1-mL fractions were collected from the top of the gradient and processed for caveolin-1 and anti-transferrin receptor (TfR) (Zymed, Invitrogen S.A.) analysis by Western blot. For phosphotyrosine residues, insulin receptor [IR], and Fyn (Santa Cruz Biotechnology), the fractions were concentrated by 10% trichloroacetic acid precipitation prior to electrophoretic analysis. Fraction proteins were measured using the BCA protein assay.

2.5. Insulin stimulation

3T3-L1 cells were cultured in medium containing 10% LPDS (control) and treated with cholesterol biosynthesis inhibitors alone or in combination with free cholesterol (30 μg/mL). Cells were serum starved for 2–4 h before insulin stimulation, which was performed in serum-free medium supplemented with 20 nM insulin (Sigma) for 10 min. Then, membranes were fractionated as mentioned before and equal volumes from gradient fractions were analyzed by Western blot. To study insulin-dependent Akt phosphorylation, cells were serum starved for 6 h, stimulated with 100 nM insulin for 20 min and collected for preparation of whole-cell lysates by using lysis buffer containing 50 mM Tris–HCl pH 7.5, 125 mM NaCl, 1% Nonidet P40, 5 mM NaF, 1.4 mM NaP pyro, 1 mM Na$_3$VO$_4$, and protease inhibitor, and used for subsequent Western blot.

2.6. Western blotting

Equal volumes of each gradient fraction or whole-cell lysates (50 μg) were subjected to 8%–12% SDS-PAGE and transferred to nitrocellulose membranes (Amersham Biosciences, Piscataway, NJ, USA). After blocking, blots were probed with specific antibodies. Horseradish peroxidase-conjugated secondary antibodies (Santa Cruz Biotechnology) were used and bands were visualized using a chemiluminescence detection system (VersaDoc, Bio-Rad). Phospho-Akt-S473 and Akt antibodies were obtained from Cell Signaling Technology Inc. (Danvers, MA, USA) and GADPH from Santa Cruz Biotechnology. To study IR phosphorylation, membranes were blotted firstly with an antibody which recognizes phosphotyrosine residues (p-Tyr) (Santa Cruz Biotechnology) and, after stripping, with an antibody against the insulin receptor [IR] β subunit (Santa Cruz Biotechnology).

2.7. Glucose uptake measurement

Prior to the assay, 3T3-L1 preadipocytes were serum deprived for 2 h in DMEM containing 0.2% BSA. Cells were incubated in the presence or absence of insulin (100 nM) at 37 °C for 30 min. The transport assay was initiated by the addition of 2-deoxy-D-glucose (1 mM final concentration), containing 0.5 mCi of 2-deoxy-D-[^{3}H] glucose (Amersham, GE Healthcare España, S.A., Barcelona, Spain) in Krebs–Ringer–Hepes buffer and incubated for 10 min at 37 °C. Then, the cells were washed 3 times in ice-cold 50 mM D-glucose in PBS. Background activity was determined by measuring the transport in a solution that contained 50 mM D-glucose. Cells were lysed with ice-cold 0.1 N NaOH-0.1% SDS and aliquots were taken for determination of [^{3}H] radioactivity. d.p.m. value was corrected by protein content in each well which was measured using a BCA protein assay kit.

2.8. Analysis of sterols by HPLC

3T3-L1 cells (175-mm flask) were incubated in 10% LPDS medium for 24 h in the absence (control) or presence of the different drugs. Sterols were extracted from either the whole-cell lysates or the fractions of the sucrose gradient and analyzed by reversed-phase HPLC, as described previously [30]. The eluted sterols were identified by comparison of the retention time and the ultraviolet spectrum against those of pure standards.

2.9. Analysis of sterol biosynthesis by HPLC

The 3T3-L1 cells were preincubated for 2 h in the absence (control) or presence of cholesterol biosynthesis inhibitors. The medium was then supplemented with 40 μCi of [14C]-acetate and incubation was prolonged 8 h further. At the end of the incubation, the cells were washed with PBS and resuspended in 10% (w/v) KOH. Then, the non-saponifiable lipids were extracted and used for sterol separation by reversed-phase HPLC, as described [31]. The eluent was monitored simultaneously by UV-absorption spectroscopy (Diodo Array 168 detector, Beckman Coulter España, S.A.) and online radioactivity counting (Radioflow detector LB 509, Berthold Technologies GmbH & Co. KG, Bad Wildbad, Germany).

2.10. Analysis of sterols by GC/MS

Extracted sterols were analyzed as described before [34]. Briefly, sterols extracted were dissolved into tert-butylmethylether (TBME) and derivatized with silylation reagent (N-methyl-N-trimethylsilyltrifluoroacetamide/Trimethylsilylimidazole 9:1). The column used was a Varian EZ Guard Factor Four 5MS 30 m × 0.25 mm × 0.25 μm (+10 m methyl deactivated guard column). The MS operated in full scan mode at 40 μamp emission current and a scan time of 0.4 s.

2.11. Analysis of phospholipids by TLC

Lipids were extracted from the fractions of the sucrose gradient with chloroform-methanol (2:1), and phospholipids were quantified following an image analysis after separation by one-dimensional thin layer chromatography [35] using the GS-800 BIOIMAGE thin layer chromatography scanner (Bio-Rad). Optical density of the spots was compared to standards on each plate and curves were drawn from second-order least-square regression equations on the standards.

2.12. Statistical analysis

Data were presented as mean ± SD. Statistical analyses were performed using a two-tailed, paired Student's *t*-test. The difference between 2 sets of values was considered significant when the *P* value was <0.05.

3. Results

3.1. Changes in sterol composition of plasma membrane domains by effect of different cholesterol biosynthesis inhibitors

To study the effects of cholesterol starvation on lipid rafts/caveolae, we incubated 3T3-L1 cells in a cholesterol-deficient medium and treated them with selected enzyme inhibitors at optimal doses for maximal inhibition of cholesterol biosynthesis. As expected, the cellular cholesterol content decreased after a 24 h treatment with each inhibitor (Supplementary Table 1); this finding is interpreted as the result of both cholesterol biosynthesis inhibition and cell division [31]. Treatment of cells with the cholesterol biosynthesis inhibitors for 24 h had no appreciable effects on cell proliferation as measured by the MTT assay (Supplementary Fig. 2). Treatment with these inhibitors also resulted in the accumulation of substrates of the inhibited enzymes (Supplementary Table 1). Thus, 3 μM SKF 104976 led to accumulation of lanosterol and dihydrolanosterol, consistent with inhibition of lanosterol 14α-demethylase [31,36]. Treatment with 5 μM AY 9944 resulted in the accumulation of 7DHC and 7-dehydrodesmosterol (7DHD), consistent with the inhibition of 3β-hydroxysterol Δ^7-reductase [31]. 5,22-Cholestadien-3β-ol (1 μg/mL) treatment led to accumulation of desmosterol and 7DHD, indicating the inhibition of Δ^{24}-reductase [30], and 3 μM triparanol resulted in the accumulation of 7DHD, zymosterol, and cholesta-8(9),14,24-trien-3β-ol, as confirmed by GC/MS analysis (Supplementary Fig. 3), indicating a strong inhibition of Δ^{24}-reductase [32] as well as inhibition of Δ^7-reductase, $\Delta^{8,7}$-isomerase, and Δ^{14}-reductase, in that order.

We next analyzed the composition of the different plasma membrane fractions. Contamination from Golgi membranes was almost completely eliminated, as assessed by β-COP immunoblotting (data not shown). Protein content in lighter fractions was very low and it sharply increased from fraction 7 to forth, fraction 9 usually having values 40 times higher than those in fractions 2 or 3 (data not shown). As regard to the lipid composition, fractions 2 and 3 were enriched in cholesterol as compared to any of the other single fractions, as these two fractions contain approximately 43% of the total cholesterol mass in the 12 membrane fractions (Supplementary Table 2). Paralleling cholesterol, fractions 2 and 3 were also enriched in sphingomyelin, by contrast, the phosphatidylcholine content was much higher in fractions 8 to 10 than in the others (Supplementary Table 2). These results are in line with those previously reported by others in different cell types [37,38], and indicate that lipid rafts/caveolae were separated in fractions 2 and 3. For the description of the results from the different experiments, data from fractions 2 and 3, representing lipid rafts/caveolae and, separately, data from fractions 8, 9, and 10, representative of the non-raft domain, were summed up (Table 1). In control cells, cholesterol content in lipid rafts was much greater (approximately 12 times) than in the non-raft fraction (Table 1). Expressed as a percentage, fractions 2 and 3 represented 40.7 ± 7.7% and fractions 8–10, 29.7 ± 6.6% of the cholesterol present in the membrane preparation. Incubation of cells with free cholesterol increased cholesterol content in both fractions to a similar extent (Table 1). Treatment with any cholesterol biosynthesis inhibitor notably decreased the cholesterol content in raft and non-raft domains (Table 1). Concomitantly, sterol precursors were incorporated into these membrane fractions. Thus, inhibition of Δ^{24}-reductase with 5,22-cholestadien-3β-ol resulted in the appearance of desmosterol and 7DHD in both membrane fractions, while zymosterol and 7DHD were detected in triparanol-treated cells (Table 1). In cells treated with SKF 104976, simultaneous supplementation with cholesterol prevented the reduction of cholesterol levels in membrane domains but did not impede the incorporation of substantial amounts of lanosterol and dihydrolanosterol into raft and non-raft fractions (Table 1). Similarly, in cells treated with AY 9944, supplementing the medium with cholesterol prevented the reduction in membrane cholesterol but only reduced in

Table 1
Effects of different cholesterol biosynthesis inhibitors on the sterol content of plasma membrane fractions.

Treatment	Cholesterol		Lanosterol		Dihydrolanosterol		7DHC		7DHD		Desmosterol		Zymosterol	
	Raft	Non-raft	Raft	Non-raft	Raft	Non-raft	Raft	Non-raft	Raft	Non-raft	Raft	Non-raft	Raft	Non-raft
Control	508 ± 118	42.9 ± 24.2	–	–	–	–	–	–	–	–	–	–	–	–
Cholesterol	699 ± 222	73.1 ± 38.5	–	–	–	–	–	–	–	–	–	–	–	–
SKF 104976	302 ± 46*	27.0 ± 5.7	27.9 ± 0.3	3.9 ± 0.5	158.0 ± 17.3	9.5 ± 1.4	–	–	–	–	–	–	–	–
SKF 104976 + cholesterol	529 ± 146	58.3 ± 30.1	17.5 ± 6.6	3.2 ± 1.1	51.2 ± 1.7	12.4 ± 6.2	–	–	–	–	–	–	–	–
AY 9944	333 ± 78*	28.2 ± 8.9	–	–	–	–	68.2 ± 1.0	2.6 ± 2.1	24.6 ± 1.2	2.7 ± 1.8	–	–	–	–
AY 9944 + cholesterol	671 ± 190**	39.8 ± 17.0	–	–	–	–	42.0 ± 2.8	1.6 ± 1.4	11.0 ± 1.1	–	–	–	–	–
5,22-cholestadien-3β-ol	257 ± 34*	17.3 ± 5.4	–	–	–	–	–	–	79.2 ± 18.8	7.7 ± 6.2	26.0 ± 3.5	2.0 ± 1.0	–	–
Triparanol	180 ± 19*	12.6 ± 2.1	–	–	–	–	–	–	30.3 ± 2.5	2.9 ± 1.1	–	–	41.0 ± 4.0	3.5 ± 1.4

3T3-L1 cells were left untreated (control) or treated for 24 h with 30 μg/mL free cholesterol and/or cholesterol biosynthesis inhibitors: 3 μM SKF 104976, 5 μM AY 9944, 1 μg/mL 5,22-cholestadien-3β-ol, or 3 μM Triparanol. Lipids were extracted from each fraction and sterols were analyzed by HPLC. Data are shown as μg of each sterol species per mg of fraction protein (raft, fractions 2 + 3; non-raft, fractions 8 + 9 + 10) (n = 3, mean ± S.D.). Comparisons vs. Control: *P<0.05; comparison of AY 9944 + Cholesterol vs. AY 9944: **P<0.05. 7DHC, 7-dehydrocholesterol; 7DHD, 7-dehydrodesmosterol; –, not detectable.

part the incorporation of intermediate sterols into membrane domains.

To explore whether the inhibition of cholesterol biosynthesis affects the polar lipid composition of raft and non-raft membrane fractions, additional experiments were performed and both sterols and phospholipids were analyzed and the results are given as Supplementary material. In general, in contrast to the sterol composition (Supplementary Table 3) treatment with the different cholesterol biosynthesis inhibitors barely affected the content of phospholipids and their distribution in any raft and non-raft fractions (Supplementary Table 4). Of interest, the total sterol/ sphingomyelin molar ratio in the raft fraction was found to be approximately 2.6 in control cells, compared to 2.5, 3.1, 2.8 and 2.4 in cells treated with SKF 104976, AY 9944, 5,22-cholestadien-3β-ol and triparanol, respectively. A subtle change in the proportions of phosphatidylinositol (increase) and phosphatidylserine (decrease) in raft fractions was observed by effect of the cholesterol biosynthesis inhibitors but the significance of this effect is elusive and further studies will be required to elucidate its biological relevance.

3.2. Colocalization of cholesterol and caveolin-1 with GM1 in the plasma membrane

Immunocytochemical studies confirmed that cholesterol, as detected by filipin staining, colocalized with GM1 in membranes from 3T3-L1 cells (Fig. 2A). Treatment with any cholesterol biosynthesis inhibitor reduced the staining for both cholesterol and GM1 and their colocalization on the cell surface, indicating decreased raft levels. To visualize GM1 and caveolin-1 we used confocal laser scanning microscopy (Fig. 2B). In untreated 3T3-L1 cells, GM1 colocalized with caveolin-1 at the plasma membrane. Inhibition of cholesterol biosynthesis resulted in a loss of both caveolin and GM1 staining at the cell surface and, interestingly, they no longer colocalized (Fig. 2B), confirming the decrease in lipid rafts/caveolae as a result of cholesterol starvation.

3.3. Cholesterol inhibition reduces caveolin-1 content in lipid rafts/caveolae

In control cells, immunoreactive caveolin-1 was mainly detected in fractions 2 and 3, indicating that these fractions contain lipid rafts/ caveolae, whereas TfR, a marker of the non-raft membrane domain, was only detected in fractions 8–11 (Fig. 3A). Inhibition of cholesterol biosynthesis with SKF 104976 resulted in a marked decrease in caveolin-1 content in fraction 2, while there was an increase in caveolin-1 in non-raft fractions (Fig. 3B). Similar results were obtained with the other inhibitors (Fig. 3C). Thus, inhibition of cholesterol biosynthesis led to a shift in the distribution of caveolin-1 from lipid rafts/caveolae to denser membrane domains. Supplementing the medium with free cholesterol prevented the effects of cholesterol biosynthesis inhibitors (Fig. 3B and 3C). Taken together with the immunocytochemical studies described above, these results indicate that cholesterol starvation disrupts lipid rafts/caveolae.
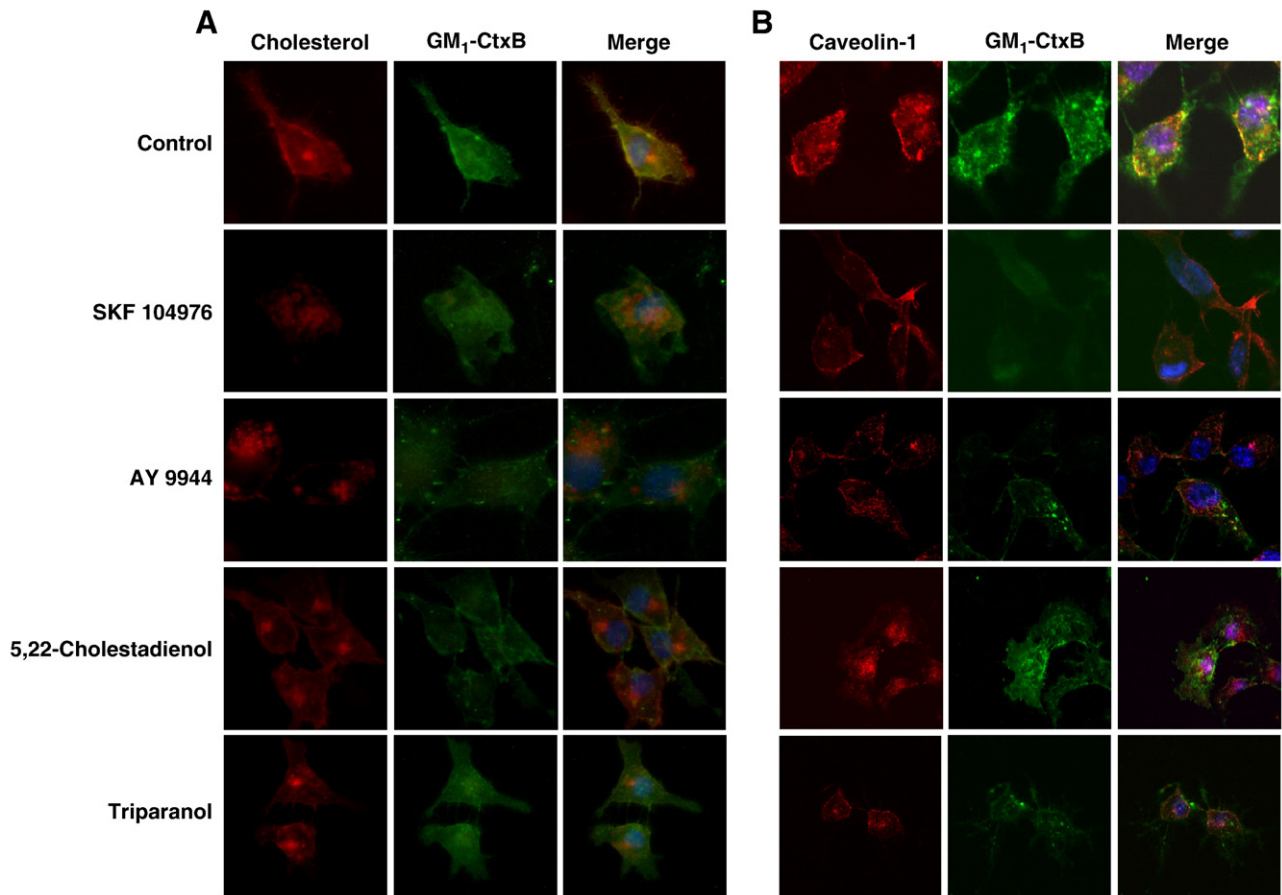

Fig. 2. Colocalization of cholesterol or caveolin-1 with GM1 in 3T3-L1 cells. Untreated cells (control) and cells treated for 24 h with 3 μM SKF 104976, 5 μM AY 9944, 1 μg/mL 5,22-cholestadien-3β-ol, or 3 μM triparanol are shown. A) Plasma membrane cholesterol was detected with filipin (red) and GM1 with CTxB-FITC (green). B) Immunocytochemistry for caveolin-1 (red) and GM1 (green). Magnification, ×400.
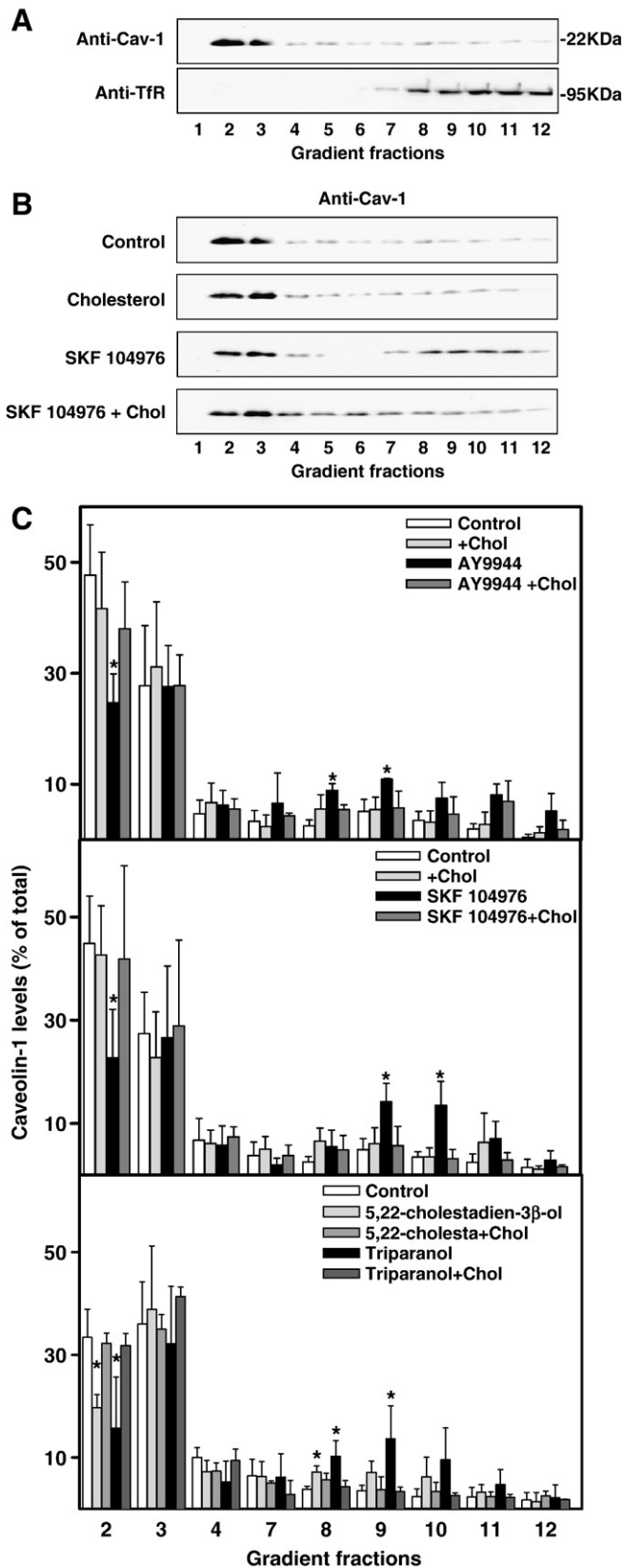
Fig. 3. Inhibition of cholesterol synthesis reduces caveolin-1 content in the lipid raft/caveolae fraction. A) Western blotting of gradient fractions with anti-caveolin-1 (Cav-1) and anti-TfR antibodies. B) Western blot with anti-caveolin-1 in 3T3-L1 cells either untreated (control) or treated with cholesterol alone (30 μg/mL), 3 μM SKF 104976 alone, or a combination of SKF 104976 and cholesterol. C) Densitometric analysis of caveolin-1 Western blots. The caveolin-1 levels are expressed as a percentage of total caveolin-1 ($n = 3$, mean ± SD). The representative results are shown in A and B. Asterisks (*) $P < 0.05$ compared with control.

3.4. Effect of cholesterol biosynthesis inhibition on insulin receptor signaling and insulin-stimulated glucose uptake

The IR is sequestered in caveolae microdomains of the plasma membrane in adipocytes through an association with caveolin, and evidence exists that caveolae are critical for insulin control [8–10]. In 3T3-L1 cells, we found that the IR β subunit was mainly detected in light, lipid raft fractions, and a similar distribution was obtained for Fyn, a Src tyrosine kinase involved in insulin signaling (Fig. 4A). To examine the effect of cholesterol starvation on IR activation, 3T3-L1 cells were treated with the cholesterol biosynthesis inhibitors alone or in combination with free cholesterol and then stimulated with insulin for the last 10 min. Cells not treated with inhibitors and not exposed to insulin were used as a control for IR activation. As shown in Fig. 4B and C, IR levels did not change significantly in response to inhibition of cholesterol biosynthesis. Addition of insulin to the incubation medium resulted in the phosphorylation of the IR (Fig. 4B). This effect was markedly lower in cells treated with cholesterol biosynthesis inhibitors than in control (+ insulin) cells. Coincubation with cholesterol restored IR activation to control values (Fig. 4B and C). Moreover, Fyn levels decreased in treated cells, an effect that was prevented by adding cholesterol to the incubation medium (Fig. 4B).

In 3T3-L1 preadipocytes, it has been shown that insulin activates phosphatidylinositol 3-kinase (PI3K)/Akt pathway, which is critical for the regulation of adipocyte differentiation [39]. As shown in Fig. 4D, insulin increased the phosphorylation of Akt-S473 in control cells. In contrast, Akt phosphorylation was markedly impaired in cells treated with cholesterol biosynthesis inhibitors, demonstrating that the coupling of IR with lipid rafts was functionally associated with insulin signaling in 3T3-L1 cells. Coincubation with cholesterol restored Akt phosphorylation to control values (Fig. 4D).

In certain cell types, insulin stimulates glucose transport. To ascertain whether cholesterol starvation affects insulin action, glucose transport was measured. As shown in Fig. 5, insulin caused a stimulation of glucose transport in 3T3-L1 preadipocytes, and all of the cholesterol biosynthesis inhibitors, SKF 104976, AY 9944 and triparanol, produced significant inhibition of the ability of insulin to enhance glucose uptake. The coincubation of the inhibitors with cholesterol restored insulin-stimulated glucose transport to control values. Just for comparison, in our system methyl β-cyclodextrin practically abrogated insulin-stimulated glucose transport, which is in accordance with previous results reported by others [8,18].

Taken together these results indicate that the lack of cholesterol impairs IR activation and intracellular signaling and that cholesterol precursors accumulating in cells treated with cholesterol biosynthesis inhibitors cannot replace cholesterol in this function.

4. Discussion

This study focused on the effects of different distal inhibitors of cholesterol biosynthesis on lipid raft/caveolae stability and signal transduction in 3T3-L1 preadipocytes. Specifically, we examined whether sterols formed during intermediate steps in cholesterol biosynthesis could substitute for cholesterol in lipid raft/caveolae formation, with the goal of defining the role of different sterols in this microdomain. For this purpose, compounds known to inhibit lanosterol 14α-demethylase, Δ^7-reductase, or Δ^{24}-reductase were tested [30–32,36]. The inhibition of cholesterol biosynthesis led to a reduction of cholesterol content in the plasma membrane and an accumulation of sterol precursors in lipid raft and non-raft domains; this was accompanied by profound alteration of lipid raft/caveolae architecture and functionality. Although sterol intermediates, especially 7DHC, were efficiently incorporated into lipid rafts and most likely contributed to membrane stability, they did not fulfill the requirements for correct protein accommodation into those signal integration platforms. The provision of sufficient cholesterol to cells
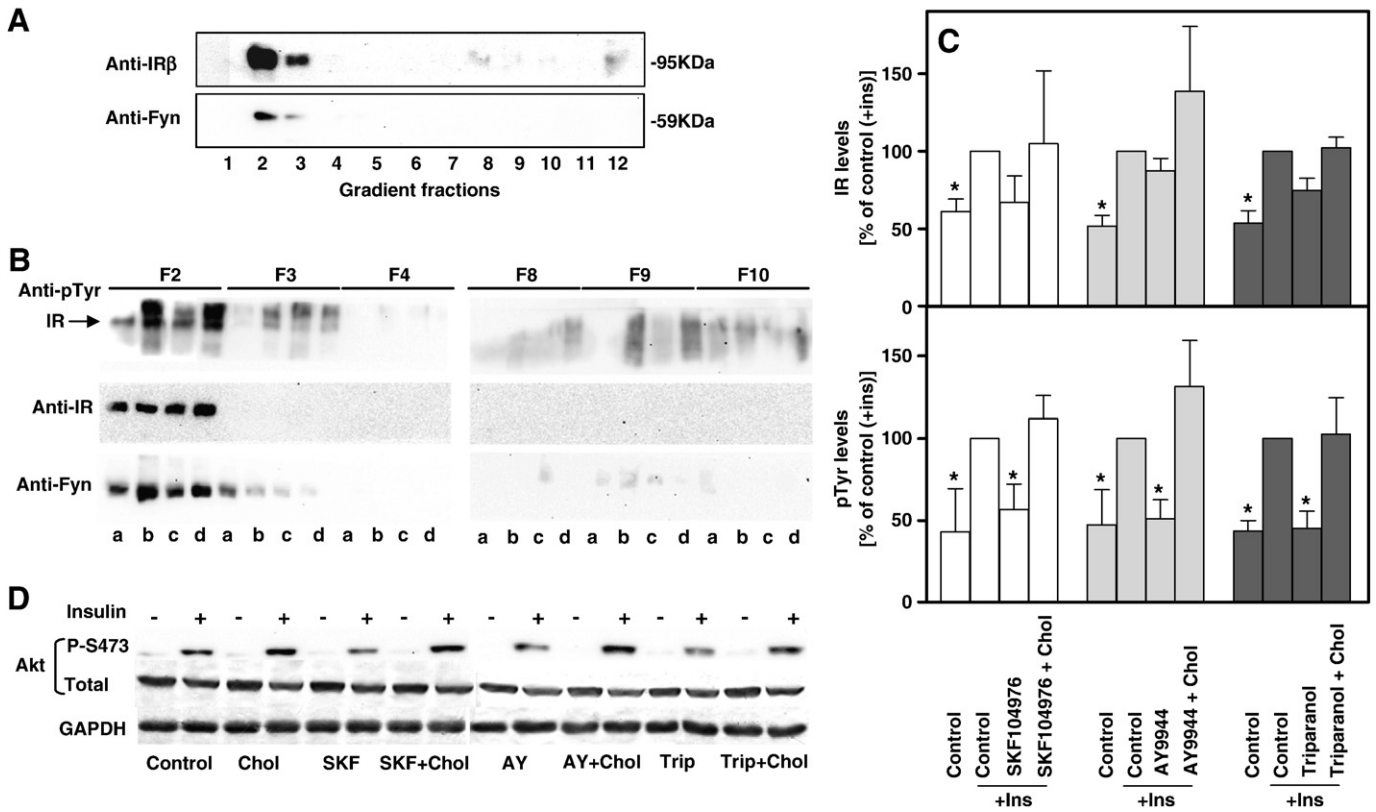
Fig. 4. Insulin receptor (IR) activation and lipid raft/caveolae association after inhibition of cholesterol biosynthesis. A) Western blotting for the IR β subunit and Fyn in gradient fractions. B) Western blotting with anti-IR, anti-pTyr (as a marker of active receptors), and anti-Fyn antibodies in untreated (control) cells (a) or cells stimulated with insulin: control + insulin (b) or treated for 24 h with 3 μM SKF 104976 alone (c) or in combination with cholesterol (d). C) Quantification of Western blots for the IR and IR activation (pTyr) ($n = 3$–4, mean ± SD). *$P < 0.05$ compared with control + insulin. D) Whole-cell lysates Western blotting using anti-phospho-Akt (p-S473), anti-Akt (total) and anti-GADPH antibodies. Ins indicates insulin; Chol, cholesterol; SKF, SKF 104976; AY, AY 9944; Trip, triparanol. Representative immunoblots are shown in A, B and D.

prevented the effects of cholesterol biosynthesis inhibitors, demonstrating the superiority of cholesterol over its immediate sterol precursors in lipid raft/caveolae function.

The inhibition of HMG-CoA reductase with statins has been shown to disrupt the distribution of signaling molecules within rafts, resulting in alterations in cell signaling [16,17]. Nonetheless, the inhibition of HMG-CoA reductase may compromise not only the provision of cholesterol but also that of non-sterol mevalonate derivatives important for cell physiology. It is currently unclear whether those effects of statins are due to impairment of raft integrity and the initial raft-dependent phosphorylation cascade or to malfunction of small GTPases due to inhibition of protein prenylation [40]. Therefore, to study the effects of cholesterol deprivation more specifically, cholesterol biosynthesis was inhibited at more distal points in the pathway. By using this approach, we herein showed, for the first time, that early sterol precursors in the cholesterol biosynthetic pathway, such as, for example, lanosterol and dehydrolanosterol, are incorporated in substitution for cholesterol into lipid rafts, where they likely contribute to sustaining the physical properties of membranes while being unable to participate in the formation of functional caveolae.

Caveolin-1 containing rafts are sensitive to cholesterol depletion [4]. Disruption of lipid rafts by the extraction of membrane cholesterol with methyl-cyclodextrins has been shown to delocalize signaling molecules and to inhibit raft-dependent signaling events [8,18,19,41]. Similarly, we found that treatment with different distal cholesterol synthesis inhibitors resulted in a shift of caveolin-1 localization in 3T3-L1 cells. Other authors reported that substitution of cholesterol by desmosterol in membranes decreases the affinity of caveolin-1 for sterol and perturbs caveolar morphology [29]. Likewise, desmosterol-reductase-deficient cells, which accumulate desmosterol instead of

cholesterol in their membranes, exhibit disrupted caveolae with markedly reduced caveolin-1 content [7]. Taken together, the results indicate that the accumulation of sterol intermediates does not compensate for the decrease in cholesterol, which shows the superiority of cholesterol in maintaining caveolae integrity.

In addition, the results of the present study in 3T3-L1 preadipocytes demonstrated that the IR is localized in caveolae purified using a detergent-free method, a finding consistent with those of previous studies in other cell types [8–10]. Insulin uses the PI3K-Akt pathway for most of its metabolic actions, such as the stimulation of glucose transport, glycogen synthesis, and lipogenesis [42]. PI3K inhibitors block adipocyte differentiation [43], and the expression of a constitutively active form of Akt is sufficient to induce adipogenesis [44]. These observations indicate that Akt represents a major PI3K effector in the insulin signaling pathway [44].

Biophysical studies have provided compelling evidence of the superiority of cholesterol over its sterol precursors [27,45]. In general, the more structurally similar a precursor is to cholesterol, the greater its capacity to maintain the biophysical properties of the membrane and the arrangement of proteins functioning within. Thus, while lanosterol, the sterol precursor most distant from cholesterol, leads to poor packing in phospholipid artificial membranes, desmosterol behaves very similarly to cholesterol in lipid packing [27]. 7DHC, the last cholesterol precursor with a saturated side-chain, has been shown to be an even stronger promoter of lipid raft domains than cholesterol [22,24], which is consistent with our observation that 7DHC preferentially localizes to raft fractions; its concentration was 27-fold greater in raft than in non-raft domains, a concentration gradient that is much steeper than found for any other sterol, including cholesterol (Table 1). Nevertheless, recent studies have demonstrated that replacement of cholesterol with either 7DHC or desmosterol
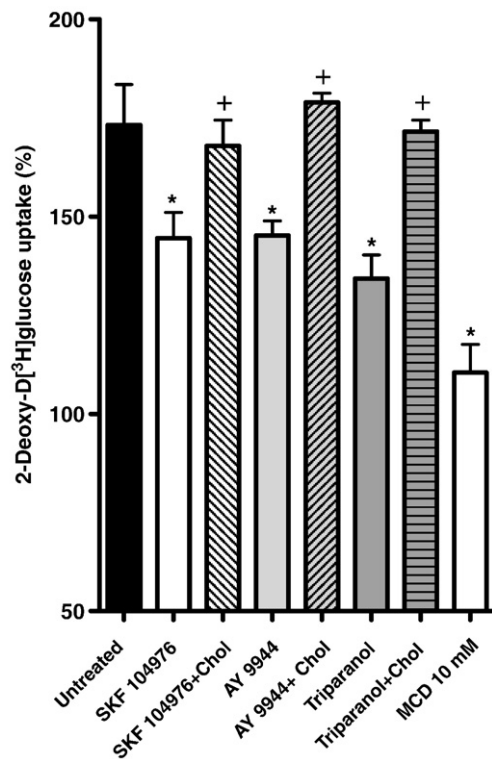
Fig. 5. Inhibition of glucose uptake by cholesterol biosynthesis inhibitors. 3T3-L1 cells were incubated without (untreated) or with cholesterol synthesis inhibitors (3 μM SKF 104976, 5 μM AY 9944 and 3 μM triparanol) or in combination with cholesterol (30 μg/ml) for 48 h, or 10 mM methyl-β-cyclodextrin (MCD) for 50 min, followed by incubation with 100 nM insulin for 30 min and the uptake of 2-deoxy-D[^{3}H]glucose was determined over 5 min. Total uptake was calculated per mg protein in the cell extract and these values were used to determine the percentage inhibition as compared to the control (not stimulated by insulin) ($n = 4$, mean ± SD). Comparisons vs. untreated *$P < 0.05$; comparison of inhibitors + cholesterol vs. inhibitor alone: †$P < 0.05$.

alters the membrane lateral pressure profile [25], a biophysical property important to membrane processes as it affects the activation of membrane proteins through changes in their conformational state [46]. In line with this, our results showed that alteration of membrane sterol composition by inhibition of cholesterol biosynthesis impairs downstream propagation of the insulin signal, as indicated by decreased phosphorylation of the IR and Akt, and uncoupling of Fyn from caveolae. Notably, the inhibition of cholesterol biosynthesis significantly inhibited insulin-stimulated glucose uptake. Previous studies by Stralfors' group reported that the extraction of membrane cholesterol by cyclodextrin abrogates the ability of insulin to enhance glucose transport [8,18], which was confirmed in the present study. Vainio et al. demonstrated that exchanging membrane cholesterol for desmosterol leads to impaired insulin receptor activation [28]. Likewise, mouse embryonic fibroblasts from DHCR24−/− mice, which are unable to synthesize cholesterol and accumulate desmosterol in membranes, exhibit impaired insulin-dependent phosphorylation of IRS-1, Akt, and Bad [7]. In addition, cells from AY 9944-treated rats or cells deficient in Δ^7-reductase have been shown to exhibit partially disrupted lipid rafts, in which Lyn kinase protein and activity are displaced [47]. Whether this latter finding is a direct effect of 7DHC, which is efficiently incorporated into these domains [26], or is due to the presence of other, accompanying sterol precursors such as 7DHD requires further investigation. In agreement with these previous reports, we found that inhibition of Δ7-reductase in 3T3-L1 preadipocytes results in the dissociation of caveolin-1 and Fyn from lipid rafts/caveolae and impairs IR autophosphorylation and insulin-dependent Akt activation. Taken together these results indicated that sterol precursors of cholesterol, while contributing to the basic

biophysical properties of membranes, are ineffective in providing the necessary environment for protein functionality in lipid rafts/caveolae, underscoring the structural specificity of cholesterol for IR functionality. It has been proposed that cholesterol directly interacts with the oxytocin receptor thereby stabilizing the receptor and modulating its binding activity [48]. Whether cholesterol similarly interacts with the IR has not been determined so far and a direct action of cholesterol on IR functionality therefore cannot be ruled out.

The superiority of cholesterol over its biosynthetic precursors was also demonstrated for other membrane receptors. It was recently reported that ligand binding and signaling of the seronotin-1A receptor, a G-protein-coupled receptor, are impaired in cells depleted of cholesterol or treated with AY 9944, and the replenishment of cholesterol but not 7DHC restores ligand binding to the receptor [49,50].

To the best of our knowledge, no study addressing the action of insulin in patients affected by congenital cholesterol biosynthesis defects has been published so far. In DHCR7-deficient mast cells, which accumulate 7DHC in lipid rafts and exhibit partially disrupted lipid rafts, Lyn kinase protein is displaced from lipid rafts and the activity of the enzyme is reduced [47]. Mouse embryonic fibroblasts from DHCR24−/− mice accumulate desmosterol in membranes and also exhibit impaired insulin signaling [7]. Regarding the effects of cholesterol biosynthesis inhibition, NB598, an inhibitor of squalene epoxidase, was recently reported to inhibit both basal and glucose-stimulated insulin secretion from mouse pancreatic islets [51]. These effects were reversed by cholesterol, similar to our results in 3T3-L1 cells. Whether dietary cholesterol is sufficient to abolish the potential alterations in insulin signaling in patients with defective cholesterol biosynthesis is not known.

The requirement for cholesterol in other cell processes, such as cell growth and division, has been recognized for many years. However, it is still unclear whether this requirement simply reflects the role of cholesterol as a membrane component or whether cholesterol also plays a regulatory role in cell functions. Previous studies by our group [52] and others [53] suggested that cholesterol exerts regulatory actions with effects on cell cycle progression. The results of this study, showing that cholesterol is required for efficient signal processing in rafts, suggest a link between membrane cholesterol and, more generally, regulatory actions in the cell.

In conclusion, the present study provides evidence of a stringent cholesterol requirement for lipid raft/caveolae stability and functionality. Sterol precursors in the cholesterol biosynthesis pathway do not maintain the insulin signaling cascade in preadipocytes. The possibility exists that fine tuning of the sterol composition in rafts by physiological changes in the activity of enzymes involved in cholesterol biosynthesis modulates the response to extracellular signals.

Acknowledgements

Appendix A. Supplementary data

Supplementary data associated with this article can be found, in the online version, at doi:10.1016/j.bbamem.2009.05.002.

References

[1] L.J. Pike, Growth factor receptors, lipid rafts and caveolae: an evolving story, Biochim. Biophys. Acta 1746 (2005) 260–273.

[2] E.J. Smart, G.A. Graf, M.A. McNiven, W.C. Sessa, J.A. Engelman, P.E. Scherer, T. Okamoto, M.P. Lisanti, Caveolins, liquid-ordered domains, and signal transduction, Mol. Cell. Biol. 19 (1999) 7289–7304.

[3] C.J. Fielding, P.E. Fielding, Cholesterol and caveolae: structural and functional relationships, Biochim. Biophys. Acta 1529 (2000) 210–222.

[4] J.P. Gratton, P. Bernatchez, W.C. Sessa, Caveolae and caveolins in the cardiovascular system, Circ. Res. 94 (2004) 1408–1417.

[5] T.M. Williams, M.P. Lisanti, Caveolin-1 in oncogenic transformation, cancer, and metastasis, Am. J. Physiol., Cell Physiol. 288 (2005) C494–C506.

[6] C.J. Fielding, P.E. Fielding, Relationship between cholesterol trafficking and signaling in rafts and caveolae, Biochim. Biophys. Acta 1610 (2003) 219–228.

[7] X. Lu, F. Kambe, X. Cao, T. Yoshida, S. Ohmori, K. Murakami, T. Kaji, T. Ishii, D. Zadworny, H. Seo, DHCR24-knockout embryonic fibroblasts are susceptible to serum withdrawal-induced apoptosis because of dysfunction of caveolae and insulin-Akt-Bad signaling, Endocrinology 147 (2006) 3123–3132.

[8] J. Gustavsson, S. Parpal, M. Karlsson, C. Ramsing, H. Thorn, M. Borg, M. Lindroth, K.H. Peterson, K.E. Magnusson, P. Stralfors, Localization of the insulin receptor in caveolae of adipocyte plasma membrane, FASEB J. 13 (1999) 1961–1971.

[9] F.H. Nystrom, H. Chen, L.N. Cong, Y. Li, M.J. Quon, Caveolin-1 interacts with the insulin receptor and can differentially modulate insulin signaling in transfected Cos-7 cells and rat adipose cells, Mol. Endocrinol. 13 (1999) 2013–2024.

[10] A. Kimura, S. Mora, S. Shigematsu, J.E. Pessin, A.R. Saltiel, The insulin receptor catalyzes the tyrosine phosphorylation of caveolin-1, J. Biol. Chem. 277 (2002) 30153–30158.

[11] R.P. Souto, G. Vallega, J. Wharton, J. Vinten, J. Tranum-Jensen, P.F. Pilch, Immunopurification and characterization of rat adipocyte caveolae suggest their dissociation from insulin signaling, J. Biol. Chem. 278 (2003) 18321–18329.

[12] M. Yamamoto, Y. Toya, C. Schwencke, M.P. Lisanti, M.G. Myers Jr., Y. Ishikawa, Caveolin is an activator of insulin receptor signaling, J. Biol. Chem. 273 (1998) 26962–26968.

[13] A.W. Cohen, B. Razani, X.B. Wang, T.P. Combs, T.M. Williams, P.E. Scherer, M.P. Lisanti, Caveolin-1-deficient mice show insulin resistance and defective insulin receptor protein expression in adipose tissue, Am. J. Physiol., Cell Physiol. 285 (2003) C222–C235.

[14] F. Capozza, T.P. Combs, A.W. Cohen, Y.R. Cho, S.Y. Park, W. Schubert, T.M. Williams, D.L. Brasaemle, L.A. Jelicks, P.E. Scherer, J.K. Kim, M.P. Lisanti, Caveolin-3 knockout mice show increased adiposity and whole body insulin resistance, with ligand-induced insulin receptor instability in skeletal muscle, Am. J. Physiol., Cell Physiol. 288 (2005) C1317–C1331.

[15] L. Liu, D. Brown, M. McKee, N.K. Lebrasseur, D. Yang, K.H. Albrecht, K. Ravid, P.F. Pilch, Deletion of Cavin/PTRF causes global loss of caveolae, dyslipidemia, and glucose intolerance, Cell. Metab. 8 (2008) 310–317.

[16] L. Zhuang, J. Kim, R.M. Adam, K.R. Solomon, M.R. Freeman, Cholesterol targeting alters lipid raft composition and cell survival in prostate cancer cells and xenografts, J. Clin. Invest. 115 (2005) 959–968.

[17] E.C. Jury, D.A. Isenberg, C. Mauri, M.R. Ehrenstein, Atorvastatin restores Lck expression and lipid raft-associated signaling in T cells from patients with systemic lupus erythematosus, J. Immunol. 177 (2006) 7416–7422.

[18] S. Parpal, M. Karlsson, H. Thorn, P. Stralfors, Cholesterol depletion disrupts caveolae and insulin receptor signaling for metabolic control via insulin receptor substrate-1, but not for mitogen-activated protein kinase control, J. Biol. Chem. 276 (2001) 9670–9678.

[19] H. Huo, X. Guo, S. Hong, M. Jiang, X. Liu, K. Liao, Lipid rafts/caveolae are essential for insulin-like growth factor-1 receptor signaling during 3T3-L1 preadipocyte differentiation induction, J. Biol. Chem. 278 (2003) 11561–11569.

[20] K. Brusselmans, L. Timmermans, T. Van de Sande, P.P. Van Veldhoven, G. Guan, I. Shechter, F. Claessens, G. Verhoeven, J.V. Swinnen, Squalene synthase, a determinant of Raft-associated cholesterol and modulator of cancer cell proliferation, J. Biol. Chem. 282 (2007) 18777–18785.

[21] W.J. Johnson, R.T. Fischer, M.C. Phillips, G.H. Rothblat, Efflux of newly synthesized cholesterol and biosynthetic sterol intermediates from cells. Dependence on acceptor type and on enrichment of cells with cholesterol, J. Biol. Chem. 270 (1995) 25037–25046.

[22] X. Xu, R. Bittman, G. Duportail, D. Heissler, C. Vilcheze, E. London, Effect of the structure of natural sterols and sphingolipids on the formation of ordered sphingolipid/sterol domains (rafts). Comparison of cholesterol to plant, fungal, and disease-associated sterols and comparison of sphingomyelin, cerebrosides, and ceramide, J. Biol. Chem. 276 (2001) 33540–33546.

[23] S. Shrivastava, Y.D. Paila, A. Dutta, A. Chattopadhyay, Differential effects of cholesterol and its immediate biosynthetic precursors on membrane organization, Biochemistry 47 (2008) 5668–5677.

[24] O. Megha, E. Bakht, London, Cholesterol precursors stabilize ordinary and ceramide-rich ordered lipid domains (lipid rafts) to different degrees. Implications for the Bloch hypothesis and sterol biosynthesis disorders, J. Biol. Chem. 281 (2006) 21903–21913.

[25] O.H. Samuli Ollila, T. Rog, M. Karttunen, I. Vattulainen, Role of sterol type on lateral pressure profiles of lipid membranes affecting membrane protein functionality: comparison between cholesterol, desmosterol, 7-dehydrocholesterol and ketosterol, J. Struct. Biol. 159 (2007) 311–323.

[26] R.K. Keller, T.P. Arnold, S.J. Fliesler, Formation of 7-dehydrocholesterol-containing membrane rafts in vitro and in vivo, with relevance to the Smith–Lemli–Opitz syndrome, J. Lipid Res. 45 (2004) 347–355.

[27] D. Huster, H.A. Scheidt, K. Arnold, A. Herrmann, P. Müller, Desmosterol may replace cholesterol in lipid membranes, Biophys. J. 88 (2005) 1838–1844.

[28] S. Vainio, M. Jansen, M. Koivusalo, T. Róg, M. Karttunen, I. Vattulainen, E. Ikonen, Significance of sterol structural specificity. Desmosterol cannot replace cholesterol in lipid rafts, J. Biol. Chem. 281 (2006) 348–355.

[29] M. Jansen, V.M. Pietiäinen, H. Pölönen, L. Rasilainen, M. Koivusalo, U. Ruotsalainen, E. Jokitalo, E. Ikonen, Cholesterol substitution increases the structural hetero-geneity of caveolae, J. Biol. Chem. 283 (2008) 14610–14618.

[30] C. Fernández, Y. Suárez, A.J. Ferruelo, D. Gómez-Coronado, M.A. Lasunción, Inhibition of cholesterol biosynthesis by Delta22-unsaturated phytosterols via competitive inhibition of sterol Delta24-reductase in mammalian cells, Biochem. J. 366 (2002) 109–119.

[31] C. Fernández, M. Martín, D. Gómez-Coronado, M.A. Lasunción, Effects of distal cholesterol biosynthesis inhibitors on cell proliferation and cell cycle progression, J. Lipid Res. 46 (2005) 920–929.

[32] G. Popjak, A. Meenan, E.J. Parish, W.D. Nes, Inhibition of cholesterol synthesis and cell growth by 24(R,S),25-iminolanosterol and triparanol in cultured rat hepatoma cells, J. Biol. Chem. 264 (1989) 6230–6238.

[33] K.S. Song, S. Li, T. Okamoto, L.A. Quilliam, M. Sargiacomo, M.P. Lisanti, Co-purification and direct interaction of Ras with caveolin, an integral membrane protein of caveolae microdomains. Detergent-free purification of caveolae microdomains, J. Biol. Chem. 271 (1996) 9690–9697.

[34] M. Giera, F. Plössl, F. Bracher, Fast and easy in vitro screening assay for cholesterol biosynthesis inhibitors in the post-squalene pathway, Steroids 72 (2007) 633–642.

[35] J.I. Ruiz, B. Ochoa, Quantification in the subnanomolar range of phospholipids and neutral lipids by monodimensional thin-layer chromatography and image analysis, J. Lipid Res. 38 (1997) 1482–1489.

[36] J. Martínez-Botas, Y. Suárez, A.J. Ferruelo, D. Gómez-Coronado, M.A. Lasunción, Cholesterol starvation decreases p34(cdc2) kinase activity and arrests the cell cycle at G2, FASEB J. 13 (1999) 1359–1370.

[37] L. Shu, L. Lee, Y. Chang, L.B. Holzman, C.A. Edwards, E. Shelden, J.A. Shayman, Caveolar structure and protein sorting are maintained in NIH 3T3 cells independent of glycosphingolipid depletion, Arch. Biochem. Biophys. 373 (2000) 83–90.

[38] S.W. Kamau, S.D. Krämer, M. Günthert, H. Wunderli-Allenspach, Effect of the modulation of the membrane lipid composition on the localization and function of P-glycoprotein in MDR1-MDCK cells, In Vitro Cell. Dev. Biol., Anim. 41 (2005) 207–216.

[39] A. Gagnon, C.S. Chen, A. Sorisky, Activation of protein kinase B and induction of adipogenesis by insulin in 3T3-L1 preadipocytes: contribution of phosphoinositide-3,4,5-trisphosphate versus phosphoinositide-3,4-bisphosphate, Diabetes 48 (1999) 691–698.

[40] R. Ghittoni, L. Patrussi, K. Pirozzi, M. Pellegrini, P.E. Lazzerini, P.L. Capecchi, F. Laghi Pasini, C.T. Baldari, Simvastatin inhibits T-cell activation by selectively impairing the function of Ras superfamily GTPases, FASEB J. 19 (2005) 605–607.

[41] M. Karlsson, H. Thorn, A. Danielsson, K.G. Stenkula, A. Ost, J. Gustavsson, F.H. Nystrom, P. Stralfors, Colocalization of insulin receptor and insulin receptor substrate-1 to caveolae in primary human adipocytes. Cholesterol depletion blocks insulin signalling for metabolic and mitogenic control, Eur. J. Biochem. 271 (2004) 2471–2479.

[42] T. Asano, M. Fujishiro, A. Kushiyama, Y. Nakatsu, H. Yoneda, H. Kamata, H. Sakoda, Role of phosphatidylinositol 3-kinase activation on insulin action and its alteration in diabetic conditions, Biol. Pharm. Bull. 30 (2007) 1610–1616.

[43] X. Xia, G. Serrero, Inhibition of adipose differentiation by phosphatidylinositol 3-kinase inhibitors, Cell Physiol. 178 (1999) 9–16.

[44] A.D. Kohn, S.A. Summers, M.J. Birnbaum, R.A. Roth, Expression of a constitutively active Akt Ser/Thr kinase in 3T3-L1 adipocytes stimulates glucose uptake and glucose transporter 4 translocation, J. Biol. Chem. 271 (1996) 31372–31378.

[45] L. Miao, M. Nielsen, J. Thewalt, J.H. Ipsen, M. Bloom, M.J. Zuckermann, O.G. Mouritsen, From lanosterol to cholesterol: structural evolution and differential effects on lipid bilayers, Biophys. J. 82 (2002) 1429–1444.

[46] P.S. Niemelä, S. Ollila, M.T. Hyvönen, M. Karttunen, I. Vattulainen, Assessing the nature of lipid raft membranes. Assessing the nature of lipid raft membranes, PLoS Comput. Biol. 3 (2007) e34.

[47] M. Kovarova, C.A. Wassif, S. Odom, K. Liao, F.D. Porter, J. Rivera, Cholesterol deficiency in a mouse model of Smith–Lemli–Opitz syndrome reveals increased mast cell responsiveness, J. Exp. Med. 203 (2006) 1161–1171.

[48] G. Gimpl, F. Fahrenholz, Cholesterol as stabilizer of the oxytocin receptor, Biochim. Biophys. Acta 1564 (2002) 384–392.

[49] A. Chattopadhyay, Y.D. Paila, M. Jafurulla, A. Chaudhuri, P. Singh, M.R. Murty, M. Vairamani, Differential effects of cholesterol and 7-dehydrocholesterol on ligand binding of solubilized hippocampal serotonin1A receptors: implications in SLOS, Biochem. Biophys. Res. Commun. 363 (2007) 800–805.

[50] Y.D. Paila, M.R. Murty, M. Vairamani, A. Chattopadhyay, Signaling by the human serotonin(1A) receptor is impaired in cellular model of Smith–Lemli–Opitz Syndrome, Biochim. Biophys. Acta. 1778 (2008) 1508–1516.

[51] F. Xia, L. Xie, A. Mihic, X. Gao, Y. Chen, H.Y. Gaisano, R.G. Tsushima, Inhibition of cholesterol biosynthesis impairs insulin secretion and voltage-gated calcium channel function in pancreatic beta-cells, Endocrinology 149 (2008) 5136–5145.

[52] Y. Suárez, C. Fernández, B. Ledo, A.J. Ferruelo, M. Martín, M.A. Vega, D. Gómez-Coronado, M.A. Lasunción, Differential effects of ergosterol and cholesterol on Cdk1 and SRE-driven transcription: sterol specificity for cell cycle progression in human cells, Eur. J. Biochem. 269 (2002) 1761–1771.

[53] M.M. Ng, F. Chang, D.R. Burgess, Movement of membrane domains and requirement of membrane signaling molecules for cytokinesis, Dev. Cell. 9 (2005) 781–790.